© 2013. Published by The Company of Biologists Ltd | Development (2013) 140, 4870-4880 doi:10.1242/dev.101725

THE COMPANY OF Biologists

RESEARCH ARTICLE

STEM CELLS AND REGENERATION

Keratin 79 identifies a novel population of migratory epithelial cells that initiates hair canal morphogenesis and regeneration

Natalia A. Veniaminova[1], Alicia N. Vagnozzi[1], Daniel Kopinke[2], Thy Thy Do[1], L. Charles Murtaugh[3], Ivan Maillard[4], Andrzej A. Dlugosz[1], Jeremy F. Reiter[2] and Sunny Y. Wong[1,*]

ABSTRACT

The formation of epithelial tubes underlies the development of diverse organs. In the skin, hair follicles resemble tube-like structures with lumens that are generated through poorly understood cellular rearrangements. Here, we show that creation of the hair follicle lumen is mediated by early outward movement of keratinocytes from within the cores of developing hair buds. These migratory keratinocytes express keratin 79 (K79) and stream out of the hair germ and into the epidermis prior to lumen formation in the embryo. Remarkably, this process is recapitulated during hair regeneration in the adult mouse, when K79$^+$ cells migrate out of the reactivated secondary hair germ prior to formation of a new hair canal. During homeostasis, K79$^+$ cells line the hair follicle infundibulum, a domain we show to be multilayered, biochemically distinct and maintained by Lrig1$^+$ stem cell-derived progeny. Upward movement of these cells sustains the infundibulum, while perturbation of this domain during acne progression is often accompanied by loss of K79. Our findings uncover previously unappreciated long-distance cell movements throughout the life cycle of the hair follicle, and suggest a novel mechanism by which the follicle generates its hollow core through outward cell migration.

KEY WORDS: Epithelial stem cells, Hair follicle, Infundibulum, Lumen, Krt79, Tube morphogenesis

INTRODUCTION

The formation of tubular structures is a morphogenetic process crucial for the development of most organs. In many polarized epithelia, tube formation is initiated by invagination of an epithelial sheet to generate a bud (Andrew and Ewald, 2010; Lubarsky and Krasnow, 2003). Subsequently, this bud can either detach from the overlying epithelium, as occurs during primary neurulation, or remain attached, as occurs during the development of lungs, kidney and pancreas. In either case, a lumen is generated as a by-product of the infolding process.

The hair follicle epithelium forms a tube-like structure that is continuous with the epidermis and houses the hair shaft (Blanpain and Fuchs, 2009; Watt and Jensen, 2009). Unlike the organs described above, developing follicles retain suprabasal cells within their cores (Andl et al., 2002; Chiang et al., 1999; Oro and Higgins, 2003; St-Jacques et al., 1998). Consequently, early hair buds do not possess lumens and require complex, and poorly characterized, cellular rearrangements to generate a hollow interior.

[1]Department of Dermatology, University of Michigan, Ann Arbor, MI 48109, USA. [2]Department of Biochemistry, University of California San Francisco, San Francisco, CA 94158, USA. [3]Department of Human Genetics, University of Utah, Salt Lake City, UT 84112, USA. [4]Life Sciences Institute, University of Michigan, Ann Arbor, MI 48109, USA.

*Author for correspondence (sunnyw@umich.edu)

Received 24 July 2013; Accepted 28 September 2013

Lumen formation is thought to be mediated by inner root sheath (IRS) cells, which extend toward the distal end of the follicle, reaching the epidermal surface concomitant with the emergence of the hair canal (Fig. 1A) (Paus et al., 1999). During the regenerative growth phase of the hair cycle (anagen), follicular morphogenesis is recapitulated, and lumen formation is also thought to be accomplished through the movement of IRS cells that ensheath the new hair shaft (Fig. 1A) (Müller-Röver et al., 2001). This hair shaft eventually erupts from the same orifice as the club hair, necessitating that the lumens of the new and old follicle fuse into a single canal. How this fusion occurs remains unclear.

In mature resting phase (telogen) hair follicles, the IRS is thought to terminate at the level of the sebaceous glands, which secrete lytic factors that cause desquamation of IRS cells (Tobin et al., 2002). Distal to the sebaceous glands is the infundibulum (INF), which encompasses the mouth of the hair follicle. Few studies have examined the INF directly; however, disruption of the INF is a hallmark of several human skin pathologies, including acne vulgaris (Bellew et al., 2011; Zaenglein et al., 2012).

Here we provide a detailed characterization of the INF and report the expression of a poorly characterized keratin, K79 (or Krt79; also known as keratin 6l), in the suprabasal cells of this domain. K79$^+$ cells are specified within the hair germ during development and in the secondary hair germ during anagen. Unexpectedly, K79$^+$ cells stream out of their respective compartments during hair follicle morphogenesis and regeneration, suggesting that early outward cell movement initiates lumen formation.

RESULTS

The hair canal is multilayered and biochemically distinct from other skin compartments

The INF comprises the mouth of the hair follicle and appears continuous with the interfollicular epidermis (IFE) and isthmus, as illustrated by immunohistochemical staining (IHC) for the basal epithelial marker keratin 5 (K5) (Fig. 1B). IHC for early (keratin 10) and late (involucrin, loricrin, filaggrin) epidermal differentiation markers also revealed multiple layers of suprabasal cells extending from the IFE into the INF, suggesting that these domains share some degree of similarity (Fig. 1B).

Previous studies have described a handful of markers for the INF, including Plet1 (also known as MTS24, 1600029D21Rik) (Nijhof et al., 2006; Raymond et al., 2010). In telogen follicles, we observed Plet1 primarily in a narrow domain between the bulge and sebaceous glands, with only occasional extension into the proximal half of the INF, as described previously (Fig. 1C). We further confirmed the localization of two additional proteins, cornifin-α (also known as Sprr1) and cystatin 6 (Cst6; also known as cystatin E/M), to the INF, although Cst6 was additionally observed in the IFE and near the upper bulge (Owens et al., 1996; Zeeuwen et al.,

Development

Development (2013) doi:10.1242/dev.101725

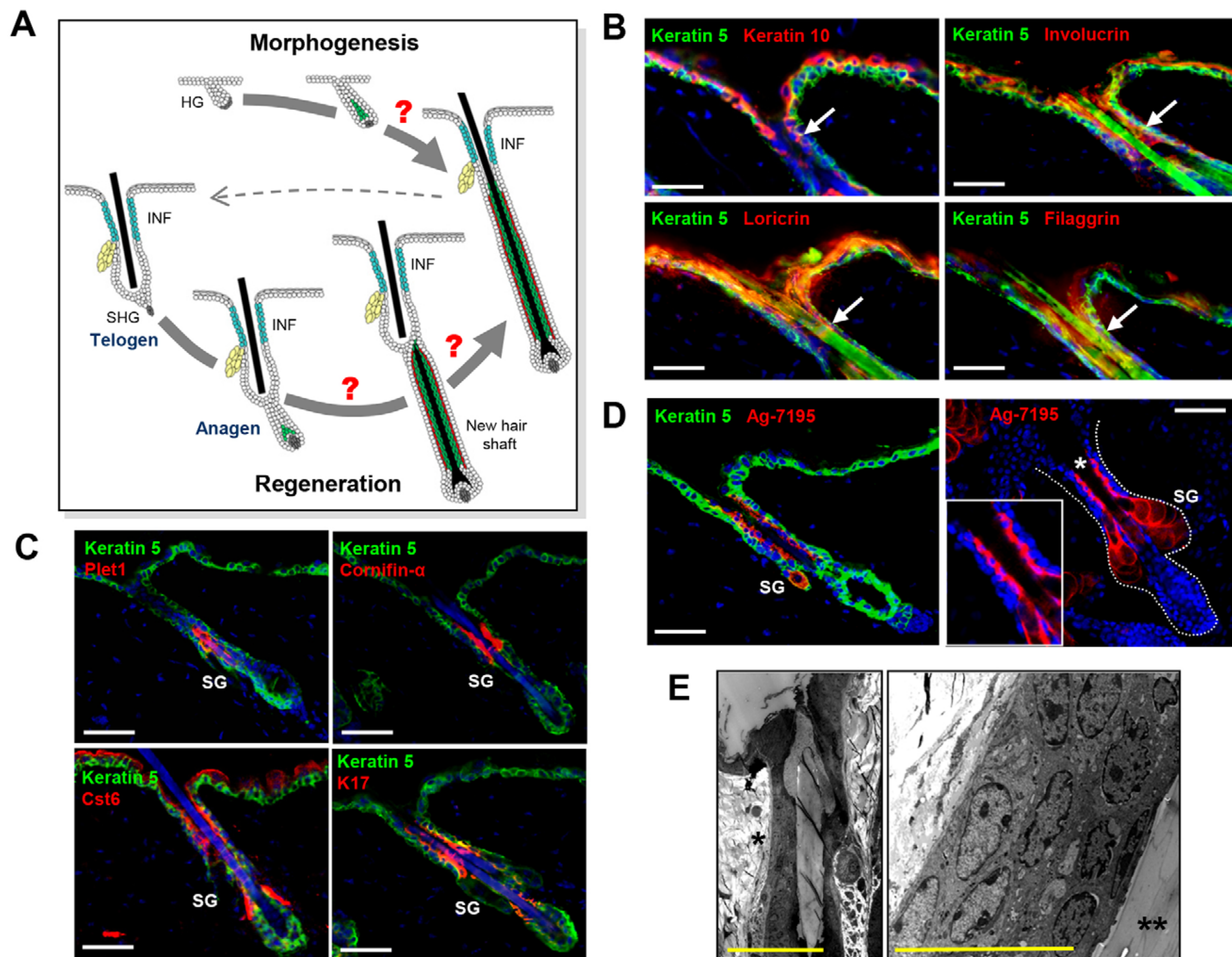

Fig. 1. The INF is multilayered and biochemically distinct. (A) Schematic summarizing hair follicle development and regeneration. The cellular mechanism for generating the hair canal lumen during morphogenesis and anagen is unclear, but is thought to involve outward movement of differentiated inner root sheath (IRS) cells (green). Note the morphological similarity between the hair germ (HG) during development and the secondary hair germ (SHG) during anagen. After generating a mature hair shaft, the follicle regresses during catagen (dashed arrow) and enters the telogen resting phase. The infundibulum (INF) (blue) remains largely unchanged throughout the adult hair cycle. Sebaceous glands, yellow; companion layer (CL), red; dermal papilla, gray. (B) Immunohistochemical staining (IHC) for various skin differentiation markers, as indicated (red). The INF basal layer, highlighted by staining for K5 (green, arrows), is continuous with the basal layer of the epidermis. (C) IHC for various markers, as indicated (red), that are enriched in the suprabasal layers of the INF (sINF) of telogen hair follicles. SG, sebaceous glands. (D) IHC using an antibody against Ag-7195 (red), as shown in standard histological sections (left) and by whole-mount (right). The asterisk indicates the region of the hair canal enlarged in the inset. (E) TEM of telogen hair follicle INF, revealing the presence of multiple layers. The asterisk indicates the region of the INF enlarged in the right panel; the hair shaft is marked by double asterisks. Scale bars: 50 μm, except 10 μm in right panel of E.

2002) (Fig. 1C). Notably, both markers are enriched in the suprabasal layers of the INF (sINF).

Over the course of our studies, we also identified novel markers of the INF. Keratin 17 (K17) is a wound-inducible protein that is expressed throughout the hair follicle (Bianchi et al., 2005; McGowan and Coulombe, 1998). We confirmed this expression pattern, but additionally observed enrichment of K17 in the sINF and upper bulge (Fig. 1C). Significantly, we found that an antibody generated against the transcription factor Gli2 strongly marks cells along the entire sINF and sebaceous glands in telogen follicles (Fig. 1D). However, IHC on embryonic day (E) 17.5 *Gli2*$^{-/-}$ skin revealed that immunostaining is maintained even in the absence of Gli2 (supplementary material Fig. S1), indicating that this antibody non-specifically recognizes an antigen, termed Ag-7195, that localizes to the sINF.

Since the formation of a multilayered epithelium is well established in the IFE but frequently overlooked in the INF, we confirmed that the INF is multilayered using transmission electron microscopy (Fig. 1E). Indeed, multiple epithelial layers were observed in the INF, with differentiating sINF cells assuming a flattened appearance. These observations indicate that, although the INF appears continuous with the IFE, sINF cells are biochemically distinct from other compartments in the skin.

K79 is expressed in the hair canal

To identify Ag-7195, we used immunoelectron microscopy to determine that this protein localizes along intermediate filaments in skin, suggesting that Ag-7195 is a keratin (Fig. 2A). In mice, the keratin family includes at least 51 members (Pan et al., 2013), of which 14 have well-characterized localization patterns distinct from that of Ag-7195. Another 15 keratins were found to be poorly expressed in telogen skin. In nearly all cases, the specialized hair keratins (K31-K40) and the IRS keratins (K25-K28, K71-K74) were

Development (2013) doi:10.1242/dev.101725

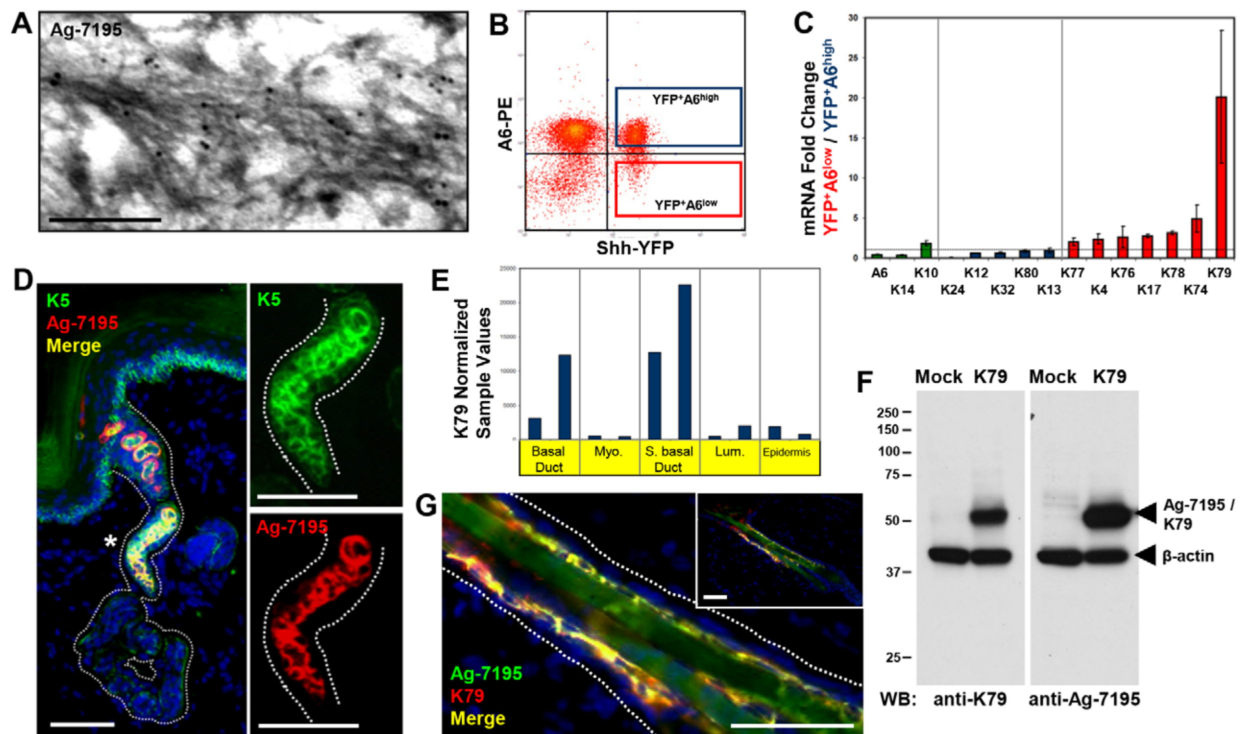

Fig. 2. Identification of K79 in the hair follicle. (A) Immunogold TEM showing that Ag-7195 localizes to keratin intermediate filaments in the skin. (B) Flow cytometry plot showing separation of hair follicle suprabasal YFP$^+$ integrin α6$^-$ cells (red box) and basal YFP$^+$ integrin α6$^+$ cells (blue box) from telogen back skin of *Shh;YFP* mice. (C) Quantitative real-time PCR analysis of various poorly characterized keratins in YFP$^+$ basal and suprabasal hair follicle cells isolated by flow cytometry in B. Values are expression fold change in suprabasal integrin α6$^-$ cells relative to basal integrin α6$^+$ cells. Green bars, expression values of well-characterized keratins (K14, K10) or integrin α6 (A6) as used to verify the proper sorting of cell populations. Blue bars, keratins displaying reduced expression in suprabasal cells. Red bars, keratins displaying increased expression in suprabasal cells. (D) IHC on sweat glands from paw skin reveals that Ag-7195 (red, left panel) is enriched in suprabasal cells lining the sweat duct. (Right) Enlarged single-channel views of the region marked by the asterisk, with DAPI omitted to enhance clarity. Although K5 (green) is typically a marker of basal cells in the skin, suprabasal sweat duct cells can also express this keratin. (E) GEO2R profile graph of K79 expression in different sweat gland compartments using data collected by Lu et al. (Lu et al., 2012). Myo, myoepithelium; s. basal, suprabasal; lum, luminal epithelium. Two replicates for each compartment were analyzed in their study and are shown here. (F) Western blot (WB) showing that both the Ag-7195 and K79 antibodies recognize overexpressed K79 in 293FT kidney epithelial cells. Blots were also probed for β-actin as a loading control. (G) IHC showing colocalization of Ag-7195 (green) and K79 (red) in the sINF (yellow, merge). Inset, low-magnification view of the same hair follicle. Error bars indicate s.e.m. Scale bars: 50 μm, except 0.25 μm in A.

expressed at low levels and were not considered further (supplementary material Table S1).

To identify keratins with a similar expression pattern to Ag-7195 in suprabasal hair follicle keratinocytes, we performed gene expression studies on purified basal (integrin α6$^+$) and suprabasal (integrin α6$^-$) hair follicle cells isolated from *Shh-Cre* mice expressing a *ROSA26R-YFP* reporter allele (*Shh;YFP*). *Shh;YFP* mice possess fluorescent hair follicles (Levy et al., 2005), which aids in the purification of these cells by flow cytometry (Fig. 2B). Of the remaining 11 keratin candidates, six (K4, K74, K76-K79) were upregulated in suprabasal YFP$^+$ integrin α6$^-$ cells, relative to basal YFP$^+$ integrin α6$^+$ cells (Fig. 2C). Importantly, *K17* was also enriched in suprabasal cells, consistent with our observation that this keratin is upregulated in the sINF (Fig. 2C).

Since the morphology of the hair follicle INF superficially resembles that of the sweat gland duct, we next assessed the localization of Ag-7195 in eccrine glands from murine paw skin. We observed that Ag-7195 is enriched specifically in the suprabasal cells lining the sweat ducts (Fig. 2D). Lu et al. recently characterized the global gene expression of the different sweat gland compartments (Lu et al., 2012), and we re-analyzed their dataset using GEO2R. Of the 39 keratins represented in their study, only K79 appeared preferentially expressed in suprabasal duct cells (Fig. 2E; supplementary material Fig. S2).

To ascertain whether the Ag-7195 antibody recognizes K79, we overexpressed this keratin in 293FT cells. Immunoblotting revealed that the Ag-7195 antibody detects a protein of the expected size for K79 in transfected cells (Fig. 2F). To confirm that K79 localizes to the sINF, we determined that an independent antibody generated specifically against K79 also demonstrates localization to the sINF and suprabasal sweat duct, but does not recognize Gli2 (Fig. 2G; supplementary material Figs S3, S4). Along with our finding that Gli2 expression is not enriched in suprabasal hair follicle cells (supplementary material Fig. S3), these data strongly suggest that the target of the Ag-7195 antibody in the INF is K79, a largely uncharacterized type II keratin that is primarily expressed in skin (Rogers et al., 2005) (supplementary material Fig. S5). To detect K79, we utilized the Ag-7195 antibody in subsequent experiments. Although we cannot rule out the possibility that this antibody can also recognize Gli2, importantly, we validated our findings using the additional K79-specific antibody as described in supplementary material Fig. S4.

The INF is maintained by Lrig1$^+$ stem cells

To identify the stem cells that give rise to the INF, we examined the localization of Lrig1, a stem cell marker that is reported to be enriched near the isthmus (Jensen et al., 2009). In telogen hair

Development (2013) doi:10.1242/dev.101725

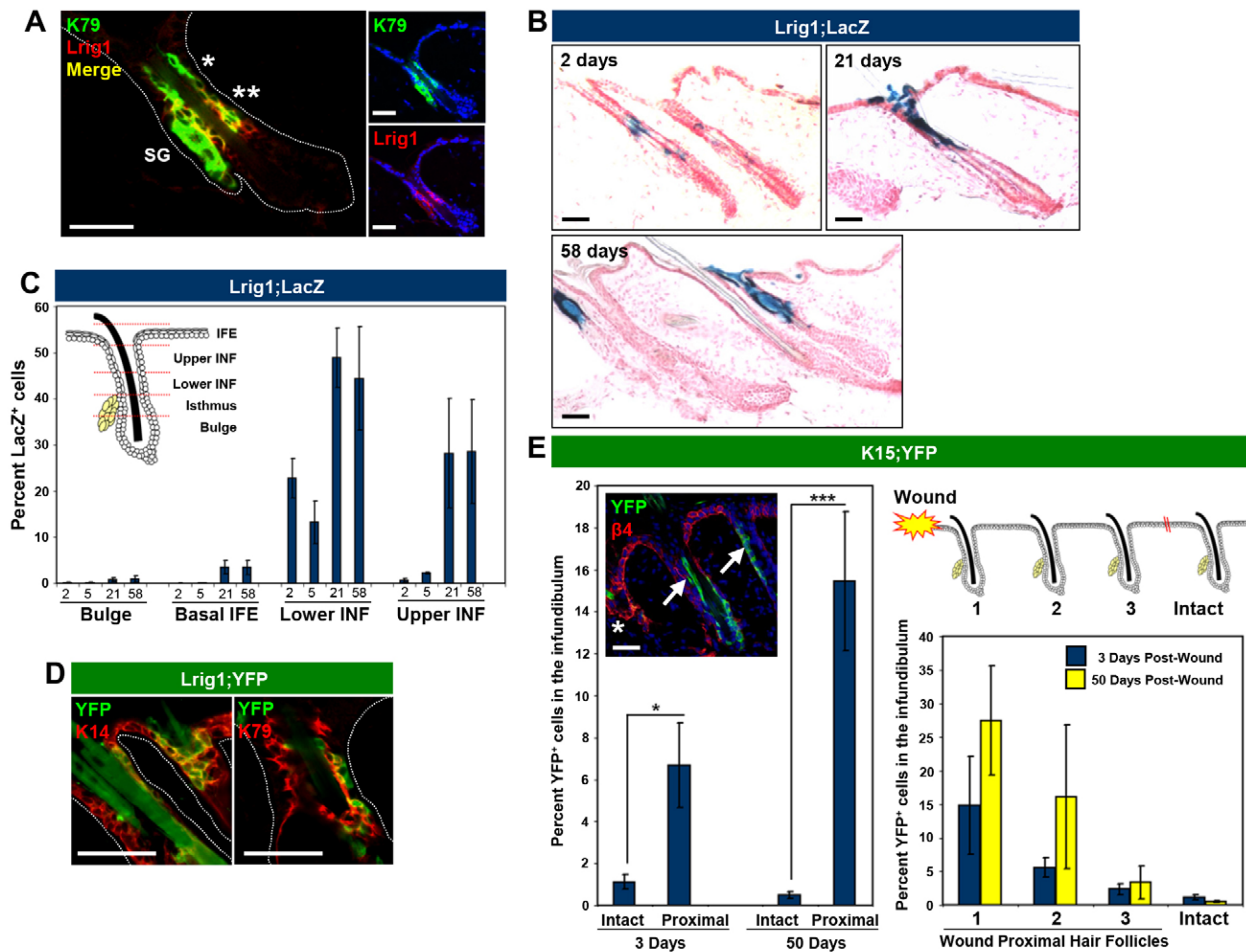

Fig. 3. The INF is sustained by Lrig1⁺ stem cells but not by bulge stem cells. (A) IHC revealing colocalization of K79 (green) and Lrig1 (red) near the hair follicle isthmus. Double asterisk marks K79 and Lrig1 double-positive cells near the isthmus; single asterisk marks K79 single-positive sINF cells extending distally beyond the isthmus. SG, sebaceous gland. DAPI was omitted to improve clarity. (Right) Single-channel views of the same follicle. (B) β-galactosidase staining of skin from *Lrig1;lacZ* mice at the indicated time points after tamoxifen induction. (C) Quantitation of lineage tracing results using *Lrig1;lacZ* mice. The average percentage labeling within each compartment is shown following a chase period of 2-58 days after tamoxifen induction, as indicated on the *x*-axis. The INF is subdivided into upper and lower half domains. IFE, interfollicular epidermis. (D) IHC showing that the progeny of Lrig1⁺ stem cells (YFP, green) contributes stably to the basal (K14⁺, red, left panel) and suprabasal (K79⁺, red, right panel) layers of the INF in *Lrig1;YFP* mice, 50 days after tamoxifen induction. (E) Quantitation of bulge stem cell contribution to the INF in intact skin and in wound-proximal follicles, using *K15;YFP* mice, 3 or 50 days post injury. (Left) Wound-proximal follicles are defined as the three closest follicles to the site of wounding. Inset, example of IHC staining, depicting bulge-derived YFP⁺ cells in the INF (green, arrow), with β4-integrin as a basal layer marker (red). Asterisk indicates the wound edge. (Right) Bulge-derived contributions, by follicle, to the INF at the indicated times after wounding. The hair follicle closest to the wound site is designated as '1'. Error bars indicate s.e.m. *$P<0.05$, ***$P<0.01$; paired Student's *t*-test (*n*=6 independent skin samples per time point). Scale bars: 50 µm.

follicles, cells expressing both Lrig1 and K79 were detected at the isthmus, whereas cells expressing K79 alone were observed in the sINF (Fig. 3A).

Previous studies tracking individual cell clones have suggested that Lrig1-expressing cells contribute to the INF, IFE and sebaceous glands (Jensen et al., 2009). To examine whether Lrig1⁺ stem cells give rise to differentiated K79⁺ sINF cells, we performed lineage tracing using tamoxifen-inducible *Lrig1-Cre*^{ERT2} mice harboring either a *ROSA26R-lacZ* or *ROSA26R-YFP* reporter allele (*Lrig1;lacZ* or *Lrig1;YFP*, respectively) (Powell et al., 2012). Two days after induction with tamoxifen, *Lrig1;lacZ* mice expressed *lacZ* (β-galactosidase) near the follicular isthmus, as expected (Fig. 3B). Labeled cells contributed initially to the proximal half of the INF, before filling the entire INF over a period of 3 weeks (Fig. 3B,C). *lacZ*⁺ cells were detected in both basal and suprabasal layers of the INF, and were occasionally observed in the IFE and sebaceous glands, but rarely found in the bulge or lower anagen bulb (Fig. 3B-D; supplementary material Fig. S6). Further labeling of the INF or other compartments was not observed over longer trace periods, indicating that the replacement of unlabeled INF cells by *lacZ*-expressing progenitors in these mice had reached homeostasis (Fig. 3C; supplementary material Fig. S6).

Since hair follicle bulge stem cells have been reported to contribute to sebaceous glands (Petersson et al., 2011), we also tested the contribution of bulge cells to the INF using RU486-inducible *K15-Cre*^{PR1} mice harboring the *YFP* reporter allele (*K15;YFP*). Upon induction, *K15;YFP* mice exhibited fluorescent bulge cells; however, these cells did not contribute substantially to the INF (Fig. 3E). Wounding can mobilize bulge-derived cells to enter the IFE (Ito et al., 2005), and we observed that hair follicles adjacent to wounds also contained labeled cells in the INF (Fig. 3E). These YFP-expressing cells were maintained at least 50 days after

Development

Development (2013) doi:10.1242/dev.101725

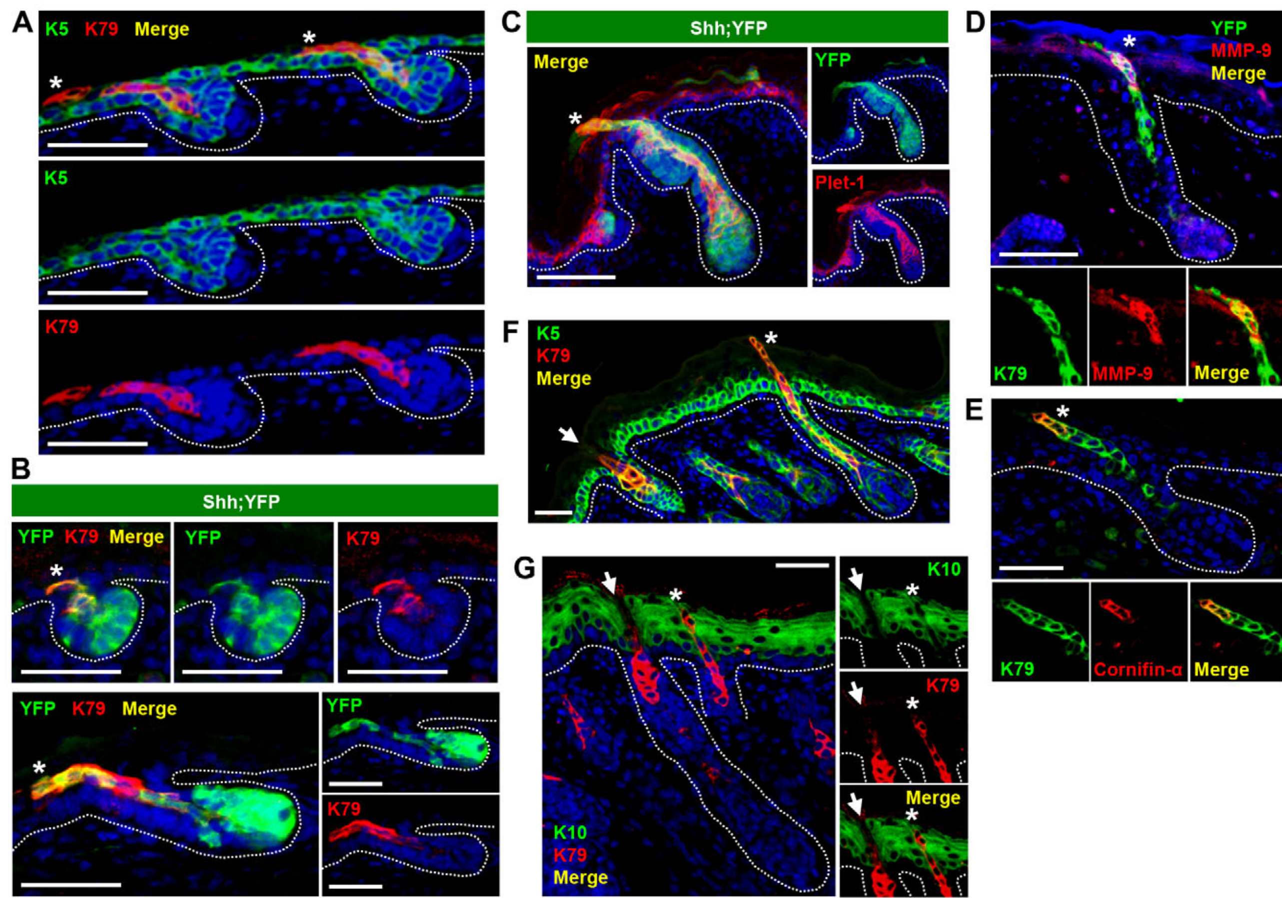

Fig. 4. Outward migration of K79⁺ cells during early hair follicle morphogenesis. (A) (Top) IHC showing that K79⁺ cells (red) form a continuous stream extending from hair germs out into the suprabasal epidermis (asterisks). The basal layer is marked by K5 (green). Beneath are single-channel views of the same hair germs. (B) Lineage tracing in *Shh;YFP* embryos reveals that K79⁺ cells (red, asterisks) are also YFP⁺ (green) and thus hair follicle derived. Note that not all hair follicle cells are YFP⁺ in *Shh;YFP* embryos, in agreement with previous observations (Levy et al., 2005). (C) Lineage tracing in *Shh;YFP* embryos reveals that Plet1⁺ cell streams (red, asterisk) are also YFP⁺ (green) and thus hair follicle derived. (D,E) IHC showing that cells at the distal tips of K79⁺ migratory streams (green) upregulate Mmp9 and cornifin-α (red). Beneath are enlarged single-channel views of the region indicated by the asterisk, with DAPI omitted to enhance clarity. (F) IHC of P3 skin, showing that K79⁺ cell streams (red) persist in some follicles (asterisk) but are lost in others (arrow). K5 marks the basal layer (green). (G) At P3, persistent K79⁺ cell streams (asterisk) frequently display weakened K10 expression (green). These streams are eventually lost from the epidermis as K79⁺ cells become restricted to the sINF, leaving behind epidermal gaps (arrow) above future hair canals. Scale bars: 50 μm.

wounding, and were in greatest abundance in follicles closest to the wound site.

Overall, our fate mapping studies reveal that the INF is ordinarily replenished by the upward movement of Lrig1⁺ stem cells, but not by bulge stem cells. Upon wounding, bulge-derived cells are mobilized up the follicle and can establish a permanent niche, probably taking on the role of departed Lrig1⁺ stem cells to stably repopulate the INF after the wound has healed. Similar findings have recently been reported by Page et al. (Page et al., 2013) and by C. Wong and A. Balmain (personal communication).

Early specification and migration of K79⁺ cells during hair follicle morphogenesis

In mice, hair follicle development initiates at E14.5. Differentiated IRS cells first appear during stage 4 of hair follicle morphogenesis, when hair pegs develop a concave follicular base that envelopes the dermal papilla (Paus et al., 1999). Subsequently, these IRS cells migrate to the top of the hair follicle during stage 6, coinciding with the emergence of the hair canal.

We examined the expression of K79 during embryogenesis, and observed the appearance of K79⁺ cells early within the hair germ (Fig. 4A). These cells were exclusively suprabasal and, surprisingly, formed a continuous stream extending from nascent hair buds into the suprabasal epidermis (Fig. 4A). These follicles were scored as stage 2 hair germs, as indicated by the absence of a concave follicular base (Paus et al., 1999). These findings suggest that the specification of cells lining the lumen of the future hair canal occurs significantly earlier than previously reported.

The appearance of K79⁺ cells extending out into the epidermis might reflect either the movement of K79⁺ cells out of the hair germ or the upregulation of K79 in a continuous column of stationary suprabasal cells. To differentiate between these possibilities, we performed lineage tracing using *Shh;YFP* embryos. Since *Shh* expression is restricted to keratinocytes fated to become hair follicles (Levy et al., 2005), all YFP⁺ keratinocytes in *Shh;YFP* embryonic epidermis must have been derived from follicles. Indeed, we observed that individual K79⁺ cells originated from within early hair germs and later formed streams that expressed YFP (Fig. 4B; supplementary material Figs S7-S9). These streams were also enriched for Plet1, K17 and K10, although expression of these markers was additionally observed outside of this domain (Fig. 4C; supplementary material Fig. S10).

Development

Development (2013) doi:10.1242/dev.101725

Importantly, in E18.5 hair pegs, cells specifically at the distal tips of migratory streams upregulated cornifin-α as well as the matrix metalloproteinase Mmp9 (Fig. 4D,E). Sharov et al. previously noted the appearance of Mmp9$^+$ cells above the presumptive hair canal (Sharov et al., 2011). K79$^+$ cell streams persisted until approximately postnatal day (P) 3 and displayed weakened expression of K10 (Fig. 4F,G). In more mature follicles, K79$^+$ cells were lost from the epidermis and became restricted to the sINF, leaving behind gaps in the epidermis above sites of future hair canals (Fig. 4G). These findings suggest a novel mechanism for hair follicle lumen formation, whereby K79$^+$ cells initially migrate outwards, extending from the hair germ into the epidermis. Subsequently, distal cells within K79$^+$ cell streams express proteolytic enzymes and cornification proteins, possibly serving to weaken suprabasal cell-cell junctions or to cause cellular deterioration to generate the hair follicle orifice.

Early specification and migration of K79$^+$ cells during hair follicle regeneration

Hair follicle morphogenesis is recapitulated during anagen, when the secondary hair germ (SHG) extends into the dermis to regenerate a new hair shaft (Greco et al., 2009). Similar to during development, lumen formation during regeneration is thought to be mediated by the specification and migration of IRS cells beginning in anagen III (Müller-Röver et al., 2001). By anagen IV, the tip of the IRS growth cone reaches the old hair canal, at which point the lumens of the new and old hair follicles fuse into a single cavity through an unknown mechanism.

We examined the localization of K79 in P23 hair follicles, which have re-entered anagen. Whereas K79 is not expressed in the SHG during telogen, we observed early specification of individual K79$^+$ cells in the SHGs of anagen I follicles, reminiscent of embryonic hair germs (Fig. 5A). In slightly later stage anagen follicles, streams of suprabasal K79$^+$ cells were observed along the anterior face of the club hair bulge (Fig. 5B). By mid-anagen III, these streams had formed a continuous line of K79$^+$ cells connecting the future companion layer (CL) of the new anagen follicle with the sINF of the pre-existing hair canal (Fig. 5C,D).

As in the case of embryonic hair germs, we sought to determine whether these streams involved cell movement. Brownell et al. previously demonstrated that *Gli1-Cre^{ERT2}* activates reporter expression in the upper and lower bulge/SHG in telogen follicles, with a prominent gap of unlabeled bulge cells situated between these two domains (Fig. 5E) (Brownell et al., 2011). Using *Gli1-Cre^{ERT2}* animals harboring a *YFP* reporter allele (*Gli1;YFP*), we reasoned that if K79$^+$ cells in the SHG migrate upwards into the club hair bulge, then the zone of unlabeled bulge cells during telogen would be infiltrated by YFP$^+$ cells during early anagen. To test this hypothesis, we induced *Gli1;YFP* mice with tamoxifen during telogen, depilated the skin, and examined the fate of labeled cells after 5-6 days. Individual K79$^+$ YFP$^+$ cells were observed within the SHG during anagen I (Fig. 5F; supplementary material Fig. S11), and in anagen II follicles K79$^+$ YFP$^+$ cells extended along the anterior face of the bulge (Fig. 5G; supplementary material Fig. S11). In anagen III follicles, continuous columns of K79$^+$ YFP$^+$ cells extended from the lower bulb up to the isthmus, eventually giving way to K79 single-positive cells in the sINF (Fig. 5H). Although this labeling pattern might also arise from the downward migration of labeled upper bulge cells, given that K79 expression originates in the SHG, the most parsimonious explanation for the YFP$^+$ K79$^+$ cell streams is that SHG cells migrate upwards during early anagen.

In summary, our data provide a mechanism for how the new and old hair follicle lumens fuse during regeneration. At early anagen, SHG-derived K79$^+$ cells migrate up along the anterior side of the bulge. These migratory cells terminate just below the isthmus, where they join with pre-existing K79$^+$ cells which reach up to the sINF, together generating a continuous layer of suprabasal cells that line a single lumen extending from the anagen bulb to the top of the hair canal.

K79 expression in pathological INF

To gain further insight into the regulation of K79, we examined its expression in pathological situations in which the INF is perturbed. In the skin, differentiation is mediated by Notch signaling, which is activated by cleavage events that generate the Notch receptor intracellular domain (NICD) (Schroeter et al., 1998; Watt et al., 2008). NICD subsequently translocates into the nucleus, where it forms a transcriptional complex that includes CSL/RBP-Jκ and a mastermind-like coactivator to induce the expression of target genes, including *Hes1*.

In telogen follicles, we observed nuclear NICD in the sINF, suggesting that upstream Notch signaling is activated in these cells (Fig. 6A). To confirm that downstream Notch signaling occurs in the sINF, we utilized *Hes1-Cre^{ERT2}* knock-in mice harboring either the *YFP* or *lacZ* reporter allele to monitor Notch activity (Kopinke et al., 2011). We observed YFP$^+$ cells along the sINF that disappeared within 3 weeks, consistent with their rapid renewal by Lrig1$^+$ stem cells (Fig. 6B). Together, these findings suggest that the sINF consists of a transient population of cells that activate Notch.

Disruption of Notch activity in the skin, either by genetic ablation of Notch pathway components or by expression of dominant-negative GFP-tagged mastermind-like 1 (dnMAML), can induce widespread cyst formation (Blanpain et al., 2006; Demehri and Kopan, 2009; Dumortier et al., 2010; Pan et al., 2004; Proweller et al., 2006; Vauclair et al., 2005; Yamamoto et al., 2003). To determine whether Notch is required to maintain the INF, we generated mice expressing *Lrig1-Cre^{ERT2}* and a Cre-inducible *dnMAML* cassette under the control of the *ROSA26* promoter (*Lrig1;dnMAML*). Upon inducing dnMAML in adult telogen skin, the INF developed keratinized cysts specifically in the INF after 20 weeks (Fig. 6C; supplementary material Fig. S12). The progeny of Lrig1$^+$ stem cells with intact Notch signaling are normally confined to the INF (Fig. 3B), whereas dnMAML-expressing cells extended out into the epidermis (Fig. 6C), which is reminiscent of previous findings that perturbing Notch causes bulge cells to depart from their niche (Demehri and Kopan, 2009). Notably, infundibular cysts contained dnMAML-expressing K79$^+$ GFP$^+$ suprabasal cells, suggesting that canonical Notch signaling is dispensable for K79 expression.

Lastly, we examined K79 in human acne, which is characterized by perturbation of the INF (Thiboutot, 2008; Zaenglein et al., 2012). Early acne lesions develop cyst-like structures known as comedones (Fig. 6D,E), and we observed that K79 was lost in five of seven closed comedones (‘whiteheads’) removed from the faces of different patients (Fig. 6E). By contrast, all comedones retained K5, K10 and K17 (supplementary material Table S2). Although our sample size was limited, loss of K79 was generally associated with comedones that possessed larger lumenal areas. Although further studies will be needed to extend these findings, our results suggest that K79 might be lost during acne disease progression.

DISCUSSION

In polarized epithelia, tube morphogenesis is typically initiated by the infolding of a cell sheet, leading to the formation of a hollow

Development (2013) doi:10.1242/dev.101725

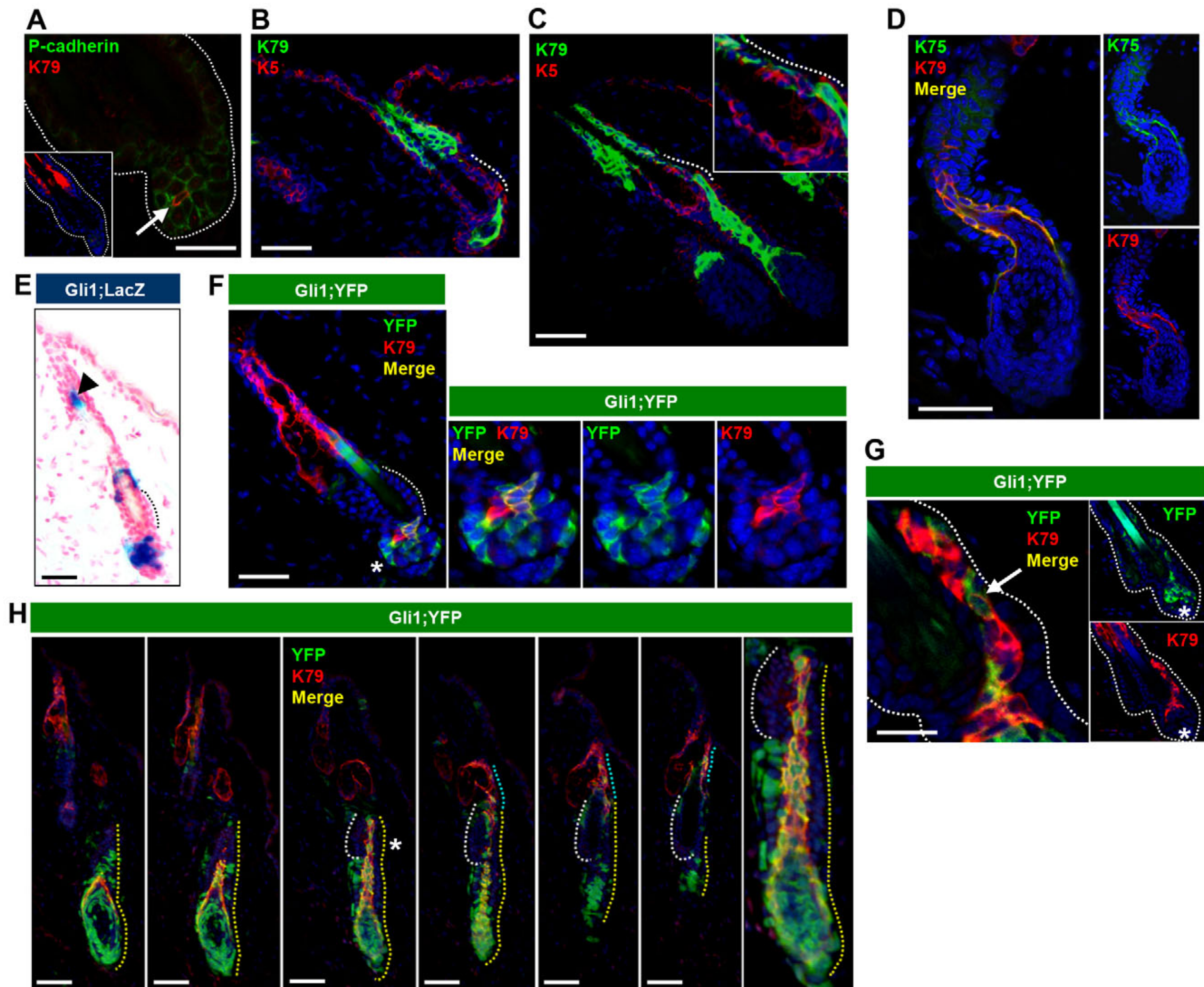

Fig. 5. Outward migration of K79$^+$ cells during early anagen. (A) IHC showing that suprabasal K79$^+$ cells (red, arrow) appear during anagen I in the SHG, which is highlighted by staining for P-cadherin (green). DAPI has been omitted to enhance clarity. Inset is a low-magnification view of the same follicle. (B) In slightly later stage anagen follicles, suprabasal K79$^+$ cells (green) extend toward the anterior face of the club hair bulge (dotted line). (C) In anagen III follicles, K79$^+$ cells have formed a continuous layer (green) extending from the anagen bulb up to the sINF. The club hair bulge, which is indicated by a dotted line along the anterior face, is magnified in the inset. (D) (Left) IHC of mature anagen follicle showing that K79 (red) localizes to the CL, as marked by K75 (green) (Gu and Coulombe, 2007). Single channels are shown to the right. (E) *Gli1;lacZ* mice display labeling of the upper bulge and SHG (blue), with a gap of unlabeled bulge cells in between (dotted line) (Brownell et al., 2011). Arrowhead indicates non-specific labeling due to endogenous β-galactosidase activity. (F) (Left) K79$^+$ cells (red) first appear in the SHG during anagen I and express YFP (green) in induced *Gli1;YFP* skin. (Right) Enlarged single-channel views of the SHG (asterisk). (G) (Left) Lineage tracing in early anagen *Gli1;YFP* skin reveals that some K79$^+$ cells (red) within the stream are also YFP$^+$ (green, arrow) and therefore likely to be derived from the SHG. (Right) Single-channel reduced magnification views of the same follicle. Asterisk indicates dermal papilla. (H) Serial sections of a later stage anagen hair follicle from depilated *Gli1;YFP* skin reveals a continuous stream of cells positive for both K79 (red) and YFP (green) extending from the bulb along the anterior face of the club hair bulge. Yellow dotted line indicates regenerated anagen follicle. White dotted line indicates club hair bulge (posterior face). Blue dotted line indicates isthmus/INF. The right-most panel is a magnified view of the region indicated by the asterisk. Scale bars: 50 μm, except 25 μm in A,G.

lumen. Hair follicle primordia also invaginate into the dermis during development, but uniquely maintain suprabasal cells in their cores that require subsequent removal. Our observation that these cells migrate out of nascent hair germs prior to lumen formation suggests a unique mechanism for hair canal morphogenesis, a process that has remained poorly studied.

Indeed, early anatomical studies have suggested a variety of mechanisms for lumen formation. In the opossum, Gibbs observed that a plug of cells connected to the sebaceous glands is initially pushed into the epidermis (Gibbs, 1938). Subsequently, these cells deflect horizontally beneath the stratum corneum before keratinizing to form the canal. A similar mechanism has also been described in sheep (Wildman, 1932). By contrast, using mouse skin explants, Hardy suggested that hair canal morphogenesis begins with the keratinization of cells within the stratum spinosum of the epidermis (Hardy, 1949). This mechanism has also been proposed for canal formation in human skin (Maximow and Bloom, 1934).

In mice, the earliest sign of hair canal specification is thought to occur during stage 3 of hair follicle morphogenesis, when epidermal keratinocytes above the hair bud appear to reorient perpendicularly to the skin surface (Pinkus, 1958). By contrast, we show here that

Development

Development (2013) doi:10.1242/dev.101725

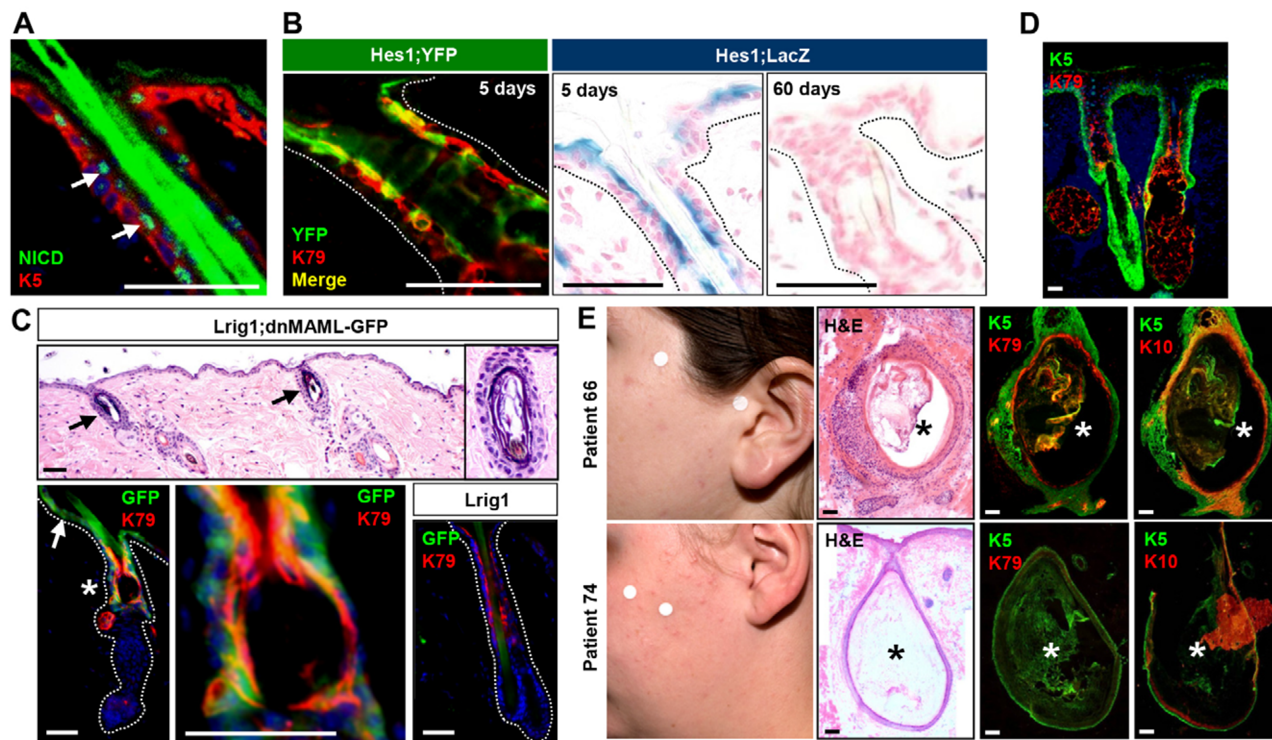

Fig. 6. Expression of K79 in pathological INF. (A) IHC for cleaved Notch receptor intracellular domain (NICD) (green, arrows) in the sINF. (B) IHC (left) or β-galactosidase staining (middle and right) showing the localization of labeled cells from *Hes1;YFP* (green) or *Hes1;lacZ* (blue) mice at the indicated time points after tamoxifen induction. (C) (Top) Hematoxylin and Eosin (H&E) staining of hair follicles containing cystic INF domains (arrows) from *Lrig1;dnMAML* skin, 20 weeks after tamoxifen induction. (Bottom left) IHC for dnMAML-GFP (green) and K79 (red). Asterisk indicates cystic region in the INF. Arrow indicates progeny of Lrig1$^+$ stem cells expressing dnMAML that have migrated into the epidermis. (Bottom middle) Enlarged view of the region indicated by the asterisk. (Bottom right) Hair follicle from littermate control animal. (D) IHC for K5 (green) and K79 (red) in normal human hair follicles. (E) (Left) Facial acne from two patients. (Middle) H&E staining of acne comedones removed from patients 66 and 74. (Right) IHC for K79 (red) and other differentiation markers, as indicated, in serial sections of the same comedones as stained by H&E. The comedone from patient 66 retained K79, whereas the comedone from patient 74 lost K79. DAPI has been omitted to enhance clarity. Asterisk indicates comedonal cyst. Scale bars: 50 µm.

by stage 2 the nascent follicles already possess continuous streams of hair germ-derived K79$^+$ cells extending out into the epidermis. In later stage hair pegs, the tips of these streams upregulate Mmp9, suggesting that the hair canal might subsequently be created through proteolysis at the distal end, leading to epidermal gaps above nascent hair follicles. Consistent with this, *Mmp9*$^{-/-}$ mice possess slightly narrower hair canals (Sharov et al., 2011); however, additional functional evidence will be needed to clarify the role of proteolysis during hair canal formation.

During early anagen, K79$^+$ streams reappear, recapitulating embryonic hair canal morphogenesis. These streams also move outwards, threading along the anterior club hair bulge and linking the future CL of the anagen follicle with pre-existing sINF cells. During homeostasis, K79$^+$ cells line the sINF, and translocate upwards over time. Although these observations suggest that migratory behavior might be a common feature of K79$^+$ cells, as supported by our lineage tracing studies using *Shh-Cre*, *Lrig1-Cre*^{ERT2} and *Gli1-Cre*^{ERT2} animals (Fig. 7), we cannot rule out the alternative possibility that these cells are passively pushed outwards.

Where do K79$^+$ cells originate from? During anagen, matrix cells give rise to the differentiated layers of the hair follicle and hair shaft, and it is possible that an early matrix cell population might also differentiate into K79$^+$ cells. However, it is important to note that K79$^+$ cells appear significantly earlier than matrix descendants such as IRS cells, both during development and regeneration. K79$^+$ cells also display outward movement earlier than do IRS cells, which are thought to extend distally only after they have ensheathed the growing hair shaft (Müller-Röver et al., 2001; Paus et al., 1999). Thus, if early, single K79$^+$ cells within the hair germ and SHG during anagen I are indeed derived from a matrix population, this would suggest that matrix cells are specified even earlier. Clearly, this is subject that deserves further study.

Since the signaling pathways that regulate K79 remain ill defined, we examined the expression of this keratin during pathological situations involving INF perturbation, both experimentally and clinically. Upon disruption of Notch, K79 is maintained, even in spite of cyst formation in the INF, suggesting that Notch signaling is unnecessary for K79 expression. By contrast, K79 is frequently lost in human acne lesions, suggesting that defective INF differentiation might be associated with disease progression. As the causes of acne are likely to be multifactorial (Thiboutot, 2008), one or several collaborating factors might contribute to downregulating K79.

Finally, although the formation of a multilayered epithelium is well established in the epidermis, the presence of multiple layers in the INF is frequently overlooked. In the opossum, Gibbs noted that although the close juxtaposition of the suprabasal layers of the hair canal and epidermis lends the appearance of continuity between these layers, these cells are, in actuality, distinct (Gibbs, 1938). We have reached a similar conclusion by examining a series of markers (K79, K17, Plet1, cornifin-α and Cst6) that we and others have found to be enriched in the sINF (Nijhof et al., 2006; Owens et al., 1996; Raymond et al., 2010; Zeeuwen et al., 2002).

Development (2013) doi:10.1242/dev.101725

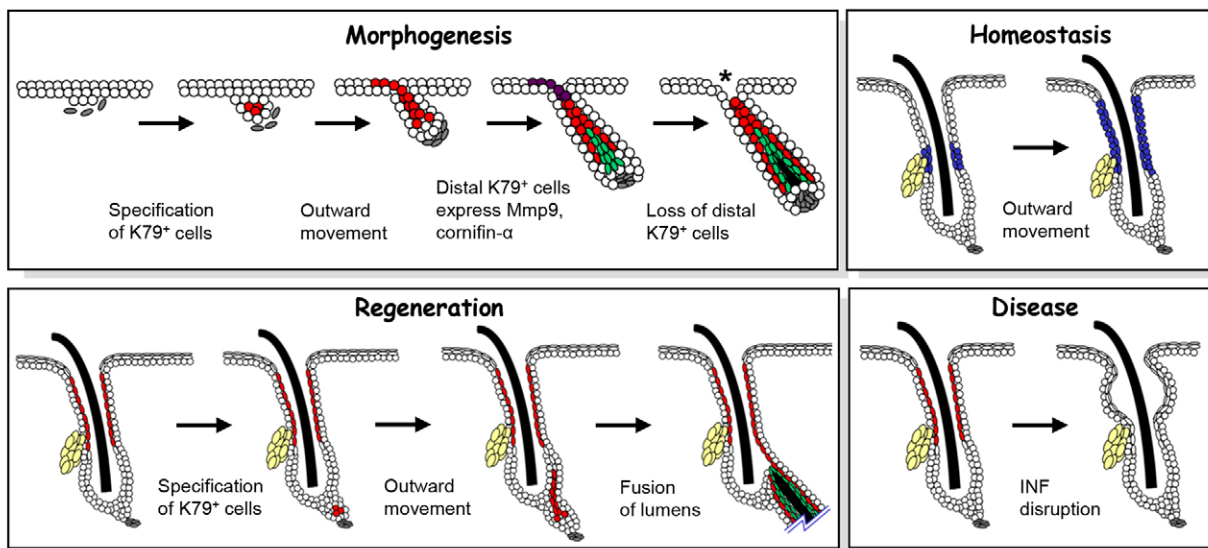

Fig. 7. Outward migration of K79⁺ cells throughout the life cycle of the hair follicle. (Top left) During hair follicle morphogenesis, K79⁺ suprabasal cells (red) are specified within hair germs and stream out into the epidermis. During the hair peg stage, cells at the distal tips of these streams (purple) upregulate Mmp9 and cornifin-α. Concomitantly at this later stage, IRS cells (green) are specified and migrate outwards from the base. K79⁺ cells are subsequently lost from the epidermis, leaving behind a gap above the future site of the hair canal (asterisk). (Bottom left) During regeneration of the follicle in early anagen, this process is recapitulated when K79⁺ cells are specified in the SHG and stream out along the anterior face of the club hair bulge. These cells eventually form a continuous layer that links the anagen CL with pre-existing K79 cells in the sINF, effectively joining the new and old hair follicle lumens. (Top right) During homeostasis, Lrig1⁺ stem cells (blue) produce progeny that move upwards over time to replenish the cells of the INF. (Bottom right) During acne vulgaris, INF differentiation is disrupted, leading to the formation of a comedone in the INF and progressive loss of K79. K79⁺ cells are in red, except in the upper right panel where Lrig1⁺ stem cells and their progeny are in blue. Not to scale.

In summary, we have identified K79 as a marker of a unique population of cells that appears to migrate throughout the life cycle of the hair follicle (Fig. 7). Future studies are likely to shed light on how K79⁺ cells sculpt the hair follicle lumen during development and how these cells are disrupted during disease.

MATERIALS AND METHODS

Mice

The following strains were used: *Lrig1*$^{tm1.1(cre/ERT2)Rj}$ (*Lrig1-Cre*^{ERT2}) (Powell et al., 2012); *Tg*$^{(Krt\text{-}15\text{-}cre/PGR)22Cot}$ (*K15-Cre*^{PR1}) (Morris et al., 2004); *Shh*$^{tm1(EGFP/cre)Cjt}$ (*Shh-Cre*) (Harfe et al., 2004); *Gli1*$^{tm3(cre/ERT2)Alj}$ (*Gli1-Cre*^{ERT2}) (Ahn and Joyner, 2004); *Hes1*$^{tm1(cre/ERT2)Lcm}$ (*Hes1-Cre*^{ERT2}) (Kopinke et al., 2011); *Gt(ROSA)26Sor*$^{tm1(EYFP)Cos}$ (*ROSA26A-YFP*) (Srinivas et al., 2001); *Gt(ROSA)26Sor*^{tm1Sor} (*ROSA26A-lacZ*) (Soriano, 1999); *ROSA26-dnMAML1-GFP* (*dnMAML*) (Tu et al., 2005); and *Gli2*$^{tm2.1Alj}$ (*Gli2*$^{-/-}$) (Bai and Joyner, 2001).

Drug induction of Cre

Mice were induced with tamoxifen or RU486 during telogen (~7.5 weeks of age) as described (Wong and Reiter, 2011) at the following doses: 5 mg tamoxifen per 40 g body weight (*Gli1-Cre*^{ERT2} and *Hes1-Cre*^{ERT2}) or 1 mg tamoxifen per 40 g body weight (*Lrig1-Cre*^{ERT2}).

Immunohistochemistry

Antibodies used for IHC included: rabbit anti-Gli2 (Ag-7195; ab7195, 1:500, Abcam); goat anti-K79 (Y-17, 1:400, Santa Cruz Biotechnology); chicken anti-GFP/YFP (GPF-1020, 1:2000, Aves Labs); guinea pig anti-K5 (GP5.2, 1:500, American Research Products); rabbit anti-K10 (PRB-159P, 1:500, Covance); rabbit anti-involucrin (PRB-140C, 1:1000, Covance); rabbit anti-loricrin (PRB-145P, 1:500, Covance); rabbit anti-filaggrin (PRB-417P, 1:1000, Covance); rat anti-Plet1 (MTS24, 1:25, gift of Dr A. Sonnenberg, The Netherlands Cancer Institute, Amsterdam, The Netherlands) (Raymond et al., 2010); rabbit anti-cornifin-α (1:250, gift of Dr A. Jetten, NIEHS, Research Triangle Park, NC, USA) (Owens et al., 1996); rabbit anti-Cst6 (ARP53533_P050, 1:25, Aviva Systems Biology); rabbit anti-K17 (4543, 1:250, Cell Signaling); goat anti-Lrig1 (AF3688, 1:20, R&D Systems); rat anti-β4 integrin (346-11A, 1:400, BD Pharmingen); rabbit anti-NICD (4147, 1:1000, Cell Signaling); rabbit anti-Mmp9 (AB19016, 1:500, Millipore); rat anti-P-cadherin (PCD-1, 1:200, Life Technologies); guinea pig anti-K75 (GPK6hf, 1:200, American Research Products); and mouse anti-K6 (LHK6B, 1:100, Lab Vision). For whole mounts, we used the protocol of Braun et al. (Braun et al., 2003).

Transmission electron microscopy (TEM)/immunogold analysis

For TEM analysis, excised skin was fixed in 3% paraformaldehyde and 2.5% glutaraldehyde in Sorensen's buffer for 90 minutes at 4°C. For immunogold analysis, skin was similarly fixed except with reduced glutaraldehyde (0.1%). Stainings were performed on standard grids, using Aurion BSA-C for blocking, Ag-7195 antibody (1:100 for 1 hour at room temperature) and donkey anti-rabbit secondary antibody conjugated to 10 nm gold particles (1:30 for 30 minutes at room temperature). Samples were post-fixed in 2% glutaraldehyde. All reagents were purchased from Electron Microscopy Sciences.

Mouse manipulations

Excision wounds and depilation on ~7.5-week-old telogen back skin were performed as previously described (Wong and Reiter, 2011). All studies were performed in accordance with regulations established by the University of Michigan Unit for Laboratory Animal Medicine.

Flow cytometry

Epidermal cells were obtained by overnight trypsinization of mouse back skin as described (Jensen et al., 2010). Cells were passed through a 40 µm cell strainer, blocked with rat anti-mouse DC16/CD32 Fc block (553141, BD Biosciences) for 5 minutes, and incubated with 50 ng Alexa 647-conjugated rat anti-human CD49f (α6 integrin) (MCA699A647T, ABD Serotec) per 1×10^6 cells for 1 hour on ice. Cells were analyzed using a MoFlo Astrios cell sorter (Beckman Coulter); $3\text{-}5\times10^4$ sorted cells were collected directly into RLT buffer (Qiagen) containing β-mercaptoethanol for RNA isolation.

RNA extraction and quantitative PCR

RNA was purified using the RNeasy Micro Kit (Qiagen) and cDNA was synthesized using the High Capacity cDNA Reverse Transcription Kit (Invitrogen). Quantitative RT-PCR was performed using Power SYBR Green PCR Master Mix (Applied Biosystems); for primers see supplementary material Table S3.

Cell culture and western blot

293FT cells were cultured in DMEM containing 10% fetal bovine serum and were transfected using Lipofectamine 2000 (Invitrogen). Mouse K79 overexpression plasmid (MMM1013-202767000) was purchased from Thermo Scientific, and pcDNA3.1-Flag-Gli2 plasmid was kindly provided by Dr M. Grachtchouk (University of Michigan). Three days after transfection, protein lysates were harvested using Laemmli buffer, resolved on 12% SDS-PAGE, and transferred to PVDF membranes, which were probed with antibodies against K79 (1:400), Ag-7195 (1:2000), FLAG (2368, 1:1000, Cell Signaling) and β-actin (A5316, 1:4000, Sigma-Aldrich).

Bioinformatics

Gene expression data from Lu et al. [accession number GSE37274 (Lu et al., 2012)] and Dezso et al. [accession number GSE7905 (Dezso et al., 2008)] were accessed through NCBI GEO2R. Data visualization was performed using CIMminer.

Acne study

Human acne samples were obtained with informed consent under IRB #HUM003422 in accordance with procedures approved by the Institutional Review Board of the University of Michigan Medical School. Biopsy samples were collected for frozen sections and de-identified, and thus not regulated as per IRB guidelines.

Acknowledgements

We thank Dr R. J. Coffey (Vanderbilt University, Nashville, TN, USA) for sharing *Lrig1-Cre^{ERT2}* mice; Drs C. Wong and A. Balmain (UCSF, San Francisco, CA, USA) for distributing *Lrig1-Cre^{ERT2}* mice; Dr G. Fisher (University of Michigan, Ann Arbor, MI, USA) for human acne samples; Drs M. Grachtchouk and M. Verhaegen (University of Michigan) for sharing reagents; Dr A. M. Jetten (NIEHS, Research Triangle Park, NC, USA) for cornifin-α antibody; Dr A. Sonnenberg (The Netherlands Cancer Institute, Amsterdam, The Netherlands) for Plet1 antibody; and Laura Melroy (Santa Cruz Biotechnology) for K79 antibody.

Competing interests

The authors declare no competing financial interests.

Author contributions

N.A.V. and S.Y.W. conceived and performed experiments, wrote the manuscript and secured funding. A.N.V. and T.T.D. performed experiments. D.K. and L.C.M. shared reagents. I.M., A.A.D. and J.F.R. shared reagents and provided feedback.

Funding

S.Y.W. acknowledges the support of the National Institutes of Health/NIAMS [R00AR059796]; the University of Michigan Department of Dermatology; the Biological Sciences Scholars Program; and the Center for Organogenesis. J.F.R. acknowledges support from the NIH [R01AR054396, R01GM095941]; the Burroughs Wellcome Fund; the Packard Foundation; and the Sandler Family Supporting Foundation. A.A.D. acknowledges support from the NIH [R01AR045973]. Deposited in PMC for release after 12 months.

Supplementary material

Supplementary material available online at
http://dev.biologists.org/lookup/suppl/doi:10.1242/dev.101725/-/DC1

References

Ahn, S. and Joyner, A. L. (2004). Dynamic changes in the response of cells to positive hedgehog signaling during mouse limb patterning. *Cell* **118**, 505-516.

Andl, T., Reddy, S. T., Gaddapara, T. and Millar, S. E. (2002). WNT signals are required for the initiation of hair follicle development. *Dev. Cell* **2**, 643-653.

Andrew, D. J. and Ewald, A. J. (2010). Morphogenesis of epithelial tubes: Insights into tube formation, elongation, and elaboration. *Dev. Biol.* **341**, 34-55.

Bai, C. B. and Joyner, A. L. (2001). Gli1 can rescue the in vivo function of Gli2. *Development* **128**, 5161-5172.

Bellew, S., Thiboutot, D. and Del Rosso, J. Q. (2011). Pathogenesis of acne vulgaris: what's new, what's interesting and what may be clinically relevant. *J. Drugs Dermatol.* **10**, 582-585.

Bianchi, N., Depianto, D., McGowan, K., Gu, C. and Coulombe, P. A. (2005). Exploiting the keratin 17 gene promoter to visualize live cells in epithelial appendages of mice. *Mol. Cell Biol.* **25**, 7249-7259.

Blanpain, C. and Fuchs, E. (2009). Epidermal homeostasis: a balancing act of stem cells in the skin. *Nat. Rev. Mol. Cell Biol.* **10**, 207-217.

Blanpain, C., Lowry, W. E., Pasolli, H. A. and Fuchs, E. (2006). Canonical notch signaling functions as a commitment switch in the epidermal lineage. *Genes Dev.* **20**, 3022-3035.

Braun, K. M., Niemann, C., Jensen, U. B., Sundberg, J. P., Silva-Vargas, V. and Watt, F. M. (2003). Manipulation of stem cell proliferation and lineage commitment: visualisation of label-retaining cells in wholemounts of mouse epidermis. *Development* **130**, 5241-5255.

Brownell, I., Guevara, E., Bai, C. B., Loomis, C. A. and Joyner, A. L. (2011). Nerve-derived sonic hedgehog defines a niche for hair follicle stem cells capable of becoming epidermal stem cells. *Cell Stem Cell* **8**, 552-565.

Chiang, C., Swan, R. Z., Grachtchouk, M., Bolinger, M., Litingtung, Y., Robertson, E. K., Cooper, M. K., Gaffield, W., Westphal, H., Beachy, P. A. et al. (1999). Essential role for Sonic hedgehog during hair follicle morphogenesis. *Dev. Biol.* **205**, 1-9.

Demehri, S. and Kopan, R. (2009). Notch signaling in bulge stem cells is not required for selection of hair follicle fate. *Development* **136**, 891-896.

Dezso, Z., Nikolsky, Y., Sviridov, E., Shi, W., Serebriyskaya, T., Dosymbekov, D., Bugrim, A., Rakhmatulin, E., Brennan, R. J., Guryanov, A. et al. (2008). A comprehensive functional analysis of tissue specificity of human gene expression. *BMC Biol.* **6**, 49.

Dumortier, A., Durham, A. D., Di Piazza, M., Vauclair, S., Koch, U., Ferrand, G., Ferrero, I., Demehri, S., Song, L. L., Farr, A. G. et al. (2010). Atopic dermatitis-like disease and associated lethal myeloproliferative disorder arise from loss of Notch signaling in the murine skin. *PLoS ONE* **5**, e9258.

Gibbs, H. F. (1938). A study of the development of the skin and hair of the Australian opossum, Trichosurus vulpecula. *Proc. Zool. Soc. Lond.* **108B**, 611-648.

Greco, V., Chen, T., Rendl, M., Schober, M., Pasolli, H. A., Stokes, N., Dela Cruz-Racelis, J. and Fuchs, E. (2009). A two-step mechanism for stem cell activation during hair regeneration. *Cell Stem Cell* **4**, 155-169.

Gu, L. H. and Coulombe, P. A. (2007). Keratin expression provides novel insight into the morphogenesis and function of the companion layer in hair follicles. *J. Invest. Dermatol.* **127**, 1061-1073.

Hardy, M. H. (1949). The development of mouse hair in vitro with some observations on pigmentation. *J. Anat.* **83**, 364-384, 3.

Harfe, B. D., Scherz, P. J., Nissim, S., Tian, H., McMahon, A. P. and Tabin, C. J. (2004). Evidence for an expansion-based temporal Shh gradient in specifying vertebrate digit identities. *Cell* **118**, 517-528.

Ito, M., Liu, Y., Yang, Z., Nguyen, J., Liang, F., Morris, R. J. and Cotsarelis, G. (2005). Stem cells in the hair follicle bulge contribute to wound repair but not to homeostasis of the epidermis. *Nat. Med.* **11**, 1351-1354.

Jensen, K. B., Collins, C. A., Nascimento, E., Tan, D. W., Frye, M., Itami, S. and Watt, F. M. (2009). Lrig1 expression defines a distinct multipotent stem cell population in mammalian epidermis. *Cell Stem Cell* **4**, 427-439.

Jensen, K. B., Driskell, R. R. and Watt, F. M. (2010). Assaying proliferation and differentiation capacity of stem cells using disaggregated adult mouse epidermis. *Nat. Protoc.* **5**, 898-911.

Kopinke, D., Brailsford, M., Shea, J. E., Leavitt, R., Scaife, C. L. and Murtaugh, L. C. (2011). Lineage tracing reveals the dynamic contribution of Hes1+ cells to the developing and adult pancreas. *Development* **138**, 431-441.

Levy, V., Lindon, C., Harfe, B. D. and Morgan, B. A. (2005). Distinct stem cell populations regenerate the follicle and interfollicular epidermis. *Dev. Cell* **9**, 855-861.

Lu, C. P., Polak, L., Rocha, A. S., Pasolli, H. A., Chen, S. C., Sharma, N., Blanpain, C. and Fuchs, E. (2012). Identification of stem cell populations in sweat glands and ducts reveals roles in homeostasis and wound repair. *Cell* **150**, 136-150.

Lubarsky, B. and Krasnow, M. A. (2003). Tube morphogenesis: making and shaping biological tubes. *Cell* **112**, 19-28.

Maximow, A. A. and Bloom, W. (1934). *A Textbook of Histology*. Philadelphia, PA: W. B. Saunders.

McGowan, K. M. and Coulombe, P. A. (1998). Onset of keratin 17 expression coincides with the definition of major epithelial lineages during skin development. *J. Cell Biol.* **143**, 469-486.

Morris, R. J., Liu, Y., Marles, L., Yang, Z., Trempus, C., Li, S., Lin, J. S., Sawicki, J. A. and Cotsarelis, G. (2004). Capturing and profiling adult hair follicle stem cells. *Nat. Biotechnol.* **22**, 411-417.

Müller-Röver, S., Handjiski, B., van der Veen, C., Eichmüller, S., Foitzik, K., McKay, I. A., Stenn, K. S. and Paus, R. (2001). A comprehensive guide for the accurate classification of murine hair follicles in distinct hair cycle stages. *J. Invest. Dermatol.* **117**, 3-15.

Nijhof, J. G., Braun, K. M., Giangreco, A., van Pelt, C., Kawamoto, H., Boyd, R. L., Willemze, R., Mullenders, L. H., Watt, F. M., de Gruijl, F. R. et al. (2006). The cell-surface marker MTS24 identifies a novel population of follicular keratinocytes with characteristics of progenitor cells. *Development* **133**, 3027-3037.

Oro, A. E. and Higgins, K. (2003). Hair cycle regulation of Hedgehog signal reception. *Dev. Biol.* **255**, 238-248.

Owens, D. M., Zainal, T. A., Jetten, A. M. and Smart, R. C. (1996). Localization and expression of cornifin-alpha/SPRR1 in mouse epidermis, anagen hair follicles, and skin neoplasms. *J. Invest. Dermatol.* **106**, 647-654.

Page, M. E., Lombard, P., Ng, F., Göttgens, B. and Jensen, K. B. (2013). The epidermis comprises autonomous compartments maintained by distinct stem cell populations. *Cell Stem Cell* **13**, 1-12.

Pan, Y., Lin, M. H., Tian, X., Cheng, H. T., Gridley, T., Shen, J. and Kopan, R. (2004). gamma-secretase functions through Notch signaling to maintain skin appendages but is not required for their patterning or initial morphogenesis. *Dev. Cell* **7**, 731-743.

Pan, X., Hobbs, R. P. and Coulombe, P. A. (2013). The expanding significance of keratin intermediate filaments in normal and diseased epithelia. *Curr. Opin. Cell Biol.* **25**, 47-56.

Paus, R., Müller-Röver, S., Van Der Veen, C., Maurer, M., Eichmüller, S., Ling, G., Hofmann, U., Foitzik, K., Mecklenburg, L. and Handjiski, B. (1999). A comprehensive guide for the recognition and classification of distinct stages of hair follicle morphogenesis. *J. Invest. Dermatol.* **113**, 523-532.

Petersson, M., Brylka, H., Kraus, A., John, S., Rappl, G., Schettina, P. and Niemann, C. (2011). TCF/Lef1 activity controls establishment of diverse stem and progenitor cell compartments in mouse epidermis. *EMBO J.* **30**, 3004-3018.

Pinkus, H. (1958). *Embryology of Hair*. New York, NY: Academic Press.

Powell, A. E., Wang, Y., Li, Y., Poulin, E. J., Means, A. L., Washington, M. K., Higginbotham, J. N., Juchheim, A., Prasad, N., Levy, S. E. et al. (2012). The pan-ErbB negative regulator Lrig1 is an intestinal stem cell marker that functions as a tumor suppressor. *Cell* **149**, 146-158.

Proweller, A., Tu, L., Lepore, J. J., Cheng, L., Lu, M. M., Seykora, J., Millar, S. E., Pear, W. S. and Parmacek, M. S. (2006). Impaired notch signaling promotes de novo squamous cell carcinoma formation. *Cancer Res.* **66**, 7438-7444.

Raymond, K., Richter, A., Kreft, M., Frijns, E., Janssen, H., Slijper, M., Praetzel-Wunder, S., Langbein, L. and Sonnenberg, A. (2010). Expression of the orphan protein Plet-1 during trichilemmal differentiation of anagen hair follicles. *J. Invest. Dermatol.* **130**, 1500-1513.

Rogers, M. A., Edler, L., Winter, H., Langbein, L., Beckmann, I. and Schweizer, J. (2005). Characterization of new members of the human type II keratin gene family and a general evaluation of the keratin gene domain on chromosome 12q13.13. *J. Invest. Dermatol.* **124**, 536-544.

Schroeter, E. H., Kisslinger, J. A. and Kopan, R. (1998). Notch-1 signalling requires ligand-induced proteolytic release of intracellular domain. *Nature* **393**, 382-386.

Sharov, A. A., Schroeder, M., Sharova, T. Y., Mardaryev, A. N., Peters, E. M., Tobin, D. J. and Botchkarev, V. A. (2011). Matrix metalloproteinase-9 is involved in the regulation of hair canal formation. *J. Invest. Dermatol.* **131**, 257-260.

Soriano, P. (1999). Generalized lacZ expression with the ROSA26 Cre reporter strain. *Nat. Genet.* **21**, 70-71.

Srinivas, S., Watanabe, T., Lin, C. S., William, C. M., Tanabe, Y., Jessell, T. M. and Costantini, F. (2001). Cre reporter strains produced by targeted insertion of EYFP and ECFP into the ROSA26 locus. *BMC Dev. Biol.* **1**, 4.

St-Jacques, B., Dassule, H. R., Karavanova, I., Botchkarev, V. A., Li, J., Danielian, P. S., McMahon, J. A., Lewis, P. M., Paus, R. and McMahon, A. P. (1998). Sonic hedgehog signaling is essential for hair development. *Curr. Biol.* **8**, 1058-1068.

Thiboutot, D. M. (2008). Overview of acne and its treatment. *Cutis* **81** Suppl., 3-7.

Tobin, D. J., Foitzik, K., Reinheckel, T., Mecklenburg, L., Botchkarev, V. A., Peters, C. and Paus, R. (2002). The lysosomal protease cathepsin L is an important regulator of keratinocyte and melanocyte differentiation during hair follicle morphogenesis and cycling. *Am. J. Pathol.* **160**, 1807-1821.

Tu, L., Fang, T. C., Artis, D., Shestova, O., Pross, S. E., Maillard, I. and Pear, W. S. (2005). Notch signaling is an important regulator of type 2 immunity. *J. Exp. Med.* **202**, 1037-1042.

Vauclair, S., Nicolas, M., Barrandon, Y. and Radtke, F. (2005). Notch1 is essential for postnatal hair follicle development and homeostasis. *Dev. Biol.* **284**, 184-193.

Watt, F. M. and Jensen, K. B. (2009). Epidermal stem cell diversity and quiescence. *EMBO Mol. Med.* **1**, 260-267.

Watt, F. M., Estrach, S. and Ambler, C. A. (2008). Epidermal Notch signalling: differentiation, cancer and adhesion. *Curr. Opin. Cell Biol.* **20**, 171-179.

Wildman, A. B. (1932). Coat and fibre development in some British sheep. *Proc. Zool. Soc. Lond.* **102**, 257-285.

Wong, S. Y. and Reiter, J. F. (2011). Wounding mobilizes hair follicle stem cells to form tumors. *Proc. Natl. Acad. Sci. USA* **108**, 4093-4098.

Yamamoto, N., Tanigaki, K., Han, H., Hiai, H. and Honjo, T. (2003). Notch/RBP-J signaling regulates epidermis/hair fate determination of hair follicular stem cells. *Curr. Biol.* **13**, 333-338.

Zaenglein, A. L., Graber, E. M. and Thiboutot, D. M. (2012). Acne vulgaris and acneiform eruptions. In *Fitzpatrick's Dermatology in General Medicine*, Vol. 1 (ed. L. A. Goldsmith, S. I. Katz, B. A. Gilchrest, A. S. Paller, D. J. Leffell and K. Wolff), pp. 897-917. Chicago, IL: McGraw Hill Medical.

Zeeuwen, P. L., van Vlijmen-Willems, I. M., Hendriks, W., Merkx, G. F. and Schalkwijk, J. (2002). A null mutation in the cystatin M/E gene of ichq mice causes juvenile lethality and defects in epidermal cornification. *Hum. Mol. Genet.* **11**, 2867-2875.

Development